Astronomical and Astrophysical Transactions (*AApTr*), 2018, Vol. 30, Issue 4, pp. 489–498,
ISSN 1055-6796, Photocopying permitted by license only, ©Cambridge Scientific Publishers

Ionospheric perturbations induced by solar X-ray flares

A. Nina*

Institute of Physics, University of Belgrade, Pregrevica 118, 11080 Belgrade, Serbia

Received 3 October, 2016

The solar X-ray flare as one of the most intensive perturbers of the atmosphere induces time variations in ionospheric plasma parameters. The intensity of these perturbations is time dependent, and they depend on the geographical location of the considered medium. Consequently, the characteristics of electromagnetic waves' propagation are time dependent and this property can be used in the diagnostics of ionospheric dynamics. This work presents an analysis of variations in plasma parameters in the ionospheric D-region during two solar X-ray flares based on monitoring the low ionosphere by the 23.4 VLF radio signal emitted in Germany and recorded in Belgrade (Serbia). We consider two C class solar X-ray flares which occurred on April 22, 2011 and were recorded by the GOES-15 satellite.

Keywords: Ionospheric D-region, solar X-ray flares, electron density, critical frequency, TEC (total electron content)

1 Introduction

As a part of the atmosphere, the ionosphere is under the permanent influence from outer space, other regions of the atmosphere and the lithosphere. For this reason, the characteristics of local plasma are time dependent as reported in numerous studies related to the electron density and changes in other plasma parameters induced by, for example, solar flares (Nina et al. 2011; Schmitter 2013), solar eclipses (Singh et al. 2011; Verhulst et al. 2016), gamma ray bursts (Nina et al. 2015a) or induced harmonic and quasi-harmonic hydrodynamic motions (including soliton formation and vortices) (Jilani et al. 2013; Nina and Čadež 2013).

Analysis of ionospheric variations is rather difficult because of space- and time-dependent variable influences arising from numerous geophysical, astrophysical and artificial events. For this reason, experimental observations play a very important role in more realistic modelling. Method selection depends on the considered altitude. Thus, in the case of the low ionosphere, there are three suitable techniques based on very low frequency (VLF) radio waves, rocket and radar measurements (Grubor et

*Email: sandrast@ipb.ac.rs

al. 2005, Strelnikova and Rapp 2010, Nina et al. 2012a, Chau et al. 2014). The first of them, which is used in this work, is based on continually emitted and recorded signals by numerous, worldwide distributed, transmitters and receivers, respectively. In addition to the detection of periodic and global low ionospheric perturbations, such an experimental setup enables registrations of sudden and unpredictable local plasma variations, for example those induced by lightning or earthquakes. The monitoring of the upper ionosphere is primarily based on measurements by ionosondes and satellite signals (Stankov et al. 2011).

Intensity of perturbations can be strongly dependent on location. One of the phenomena that induce different disturbances is a solar X-ray flare which has more intensive influence in the lower than in the upper ionosphere in daytime conditions. Namely, the electron density increase in the D-region altitude can be raised by more than one order of magnitude (Nina et al. 2012a,b, Singh et al. 2014) while, at the same time, significant variations in TEC (total electron content) are recorded only during intensive X-ray flares. Also, during a very intensive increase of X-ray radiation the height of the electron density maximum can be lowered to the E-region (Xiong et al. 2011).

In this paper we analyse changes in D-region plasma parameters induced when there are no strong solar X-ray flares that do not significantly perturb the upper ionosphere. We study electron density, electron plasma frequency and total electron content variations in the D-region during the influence of two solar X-ray flares of classes C which occurred on April 22, 2011. The data were obtained from the ionospheric monitoring by very low frequency radio signal propagation.

2 Ionospheric observations

The technique of atmospheric monitoring depends on the altitude of the considered medium. Methods to monitor the ionosphere are of two types – in situ measurements and remote sensing observations. In situ measurements can be made by rockets and they give values of local plasma parameters, and remote sensors are ground-based and in the satellites some distance away from the subject of interest. The setups for remote sensing include emitters and receivers and these observations provide integral information about the medium in which the signal propagates. The propagation path depends on the frequency of used electromagnetic waves, electron density space distribution and emission angle. If the signal propagates through the ionosphere without reflection, its frequency f must be larger than the critical frequency maximum f_{0max} that depends on electron density and emission angle. In contrast, if $f < f_{0max}$, after reflection from some ionospheric layer, the signal comes back to the ground or to the satellite.

The height of the electron density maximum and consequently of f_{0max} is in the F2-region. Because of that, the remote sensing of the D, E, F1 and lower part of F2-region can be done using an experimental setup located on the Earth's surface. Usually, very low and low frequency (VLF/LF) radio and radar signals are used for D-region monitoring (see Grubor et al. 2005, Strelnikova and Rapp 2010, Nina et al. 2011, Chau et al. 2014, Kolarski and Grubor 2014). Signals emitted by ionosondes

give information about E-, F1- and the lower part of F2-region while satellite signals can be used for observations of the upper part of the F2-region (Stankov et al. 2011).

In this paper we have used measurements based on VLF radio wave monitoring of the low ionosphere and observation of altitudes above about 100 km by ionosondes.

3 Theory and modeling

In this study we present analyses of the electron density, electron plasma frequency and total electron content in the D-region during two considered solar X-ray flares.

3.1 Electron density in the D-region

Electrons have a very significant role in various physical and chemical processes in the ionosphere. The knowledge about the electron density in space and time is needed to calculate some plasma parameter properties, for example, the effective recombination coefficient (Nina et al. 2012b), electron production and loss rate (Nina and Čadež 2014), contribution of the Lyα line influence in the ionization process at the X-ray flare intensity maximum (Nina et al. 2015b). Also, it is involved in modeling the plasma parameters such as the electron plasma frequency and index of refractivity (Bajčetić et al. 2015) needed to simulate the propagation of electromagnetic waves in the ionosphere. Consequently, research of its dynamics finds practical application in telecommunications.

In this paper, the electron density in the D-region during an X-ray flare is determined by a procedure given in Grubor et al. (2008) and is used in many other papers. This procedure is based on matching the observed VLF signal data, amplitude $\Delta A_{\rm rec}$ and phase $\Delta P_{\rm rec}$ changes, with corresponding results of simulations $\Delta A_{\rm sim}$ and $\Delta P_{\rm sim}$ of the VLF signal propagation using the Long-Wave Propagation Capability (LWPC) numerical model developed by the Naval Ocean Systems Center (NOSC), San Diego, USA (Ferguson 1998). The registered amplitude $\Delta A_{\rm rec}$ and phase $\Delta P_{\rm rec}$ changes are determined with respect to corresponding values in unperturbed conditions. In our case they are 3.0 dB and 45.6°, respectively, as seen in Fig. 1. With reference to the simulated values of amplitude and phase, they are obtained using Wait's model of the horizontally stratified ionosphere (Wait and Spies 1964) which is incorporated in the LWPC numerical model of the VLF/LF signal propagation, and is characterized by two independent parameters: the "sharpness" β and the signal reflection height H'. These parameters are the inputs for the LWPC program which then computes $A_{\rm sim}(\beta, H')$ and $P_{\rm sim}(\beta, H')$ i.e. their corresponding changes $\Delta A_{\rm sim}(\beta, H')$ and $\Delta P_{\rm sim}(\beta, H')$ as output values. Finally, the parameters β and H' are determined from the condition of best fitting the experimental data with their numerical counterparts:

$$\begin{aligned} \Delta A_{\rm sim}(\beta, H') &\approx \Delta A_{\rm rec}(t), \\ \Delta P_{\rm sim}(\beta, H') &\approx \Delta P_{\rm rec}(t). \end{aligned} \tag{1}$$

The electron density now follows from equation (Thomson 1993) as:

$$N_{\rm e}(h,t) = 1.43 \cdot 10^{13} {\rm e}^{-\beta(t)H'(t)} {\rm e}^{(\beta(t)-\beta_0)h}, \tag{2}$$

where $N_{\rm e}$ in m^{-3}, H'(t) and h are in km, β is in km^{-1} and $\beta_0 = 0.15$ km^{-1}.

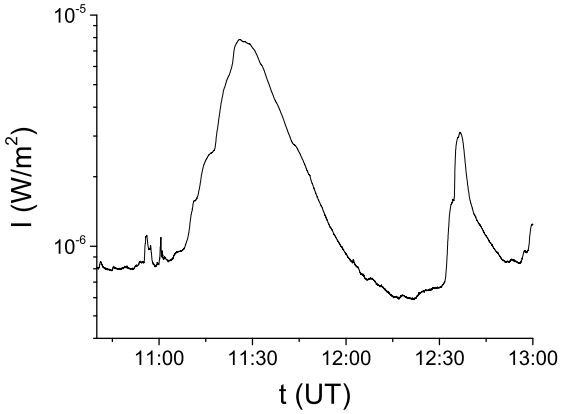


Figure 1 Time dependencies of the X radiation intensity I registered by the GOES-15 satellite in the wavelength domain between 0.1 and 0.8 nm during presence of the solar X-ray flare that occurred on April 22, 2011.

3.2 Critical frequency maxima in the E- and F-region

In the literature, the electron plasma frequency is the ionospheric parameter that is usually used for description of plasma in the E- and F-region. The relation between the electron density N_e (in m^{-3}) and plasma frequency f_0 (in Hz) in the ionosphere can be expressed by the approximative relation:

$$f_0(h,t) \approx 8.98\sqrt{N_e(h,t)}. \tag{3}$$

Here we present relative changes of f_0 during perturbation with respect to the quiet state (t_q) in the D-region:

$$\delta f_0(h,t) = \frac{f_0(h,t) - f_0(h,t_q)}{f_0(h,t_q)}. \tag{4}$$

3.3 Total electron content (TEC)

The total electron content (TEC) is one of the most important parameters that describes the ionospheric state and structure and provides an overall reflection of ionization processes. It is the column electron number density defined as the number of free electrons in a column of unit cross section practically extending from the bottom h_b to the top h_t of the ionosphere:

$$\mathrm{TEC}(t) = \int_{h_\mathrm{g}}^{h_\mathrm{t}} N_\mathrm{e}(h,t)dh. \tag{5}$$

In addition to scientific research (see, for example, Afraimovich et al. 2009) TEC is used in calculations needed for practical applications in telecommunication (for example in systems which use transionospheric radio waves, Hofmann-Wellenhof et al. 2001) and in global navigation satellite systems (GNSS, Jakowski et al. 2005).

Keeping in mind that radio communications, positioning, navigation and timing by GNSS signals play a critical role in telecommunications, geodesy and land surveying, emergency response, precision agriculture, all forms of transportation (space stations, aviation, maritime, rail, road and mass transit), the studies of relevant signal propagations and consequently TEC are of great importance at the present time.

TEC measurements are made mostly using the GNSS data because of a good global coverage of the GNSS observation network (Shim 2009). However, TEC can be calculated from electron densities obtained by different methods depending on altitude (see Section 2). Here, we restrict the altitude domain considered in calculation on the D-region.

4 Results and discussion

In this study we analysed ionospheric disturbances induced by two solar X-flares which occurred on April 22, 2011 with photon flux I registered by the GOES-15 satellite of National Oceanic and Atmospheric Administration (NOAA), USA (Fig. 1) at wavelength range 0.1–0.8 nm.

The D-region perturbations were detected as amplitude $\Delta A_{\rm rec}$ and phase $\Delta P_{\rm rec}$ variations of the considered VLF signal recorded by the AWESOME (Atmospheric Weather Electromagnetic System for Observation Modelling and Education) VLF receiver (Cohen et al. 2010) (Fig. 2, upper and bottom panels, respectively). We

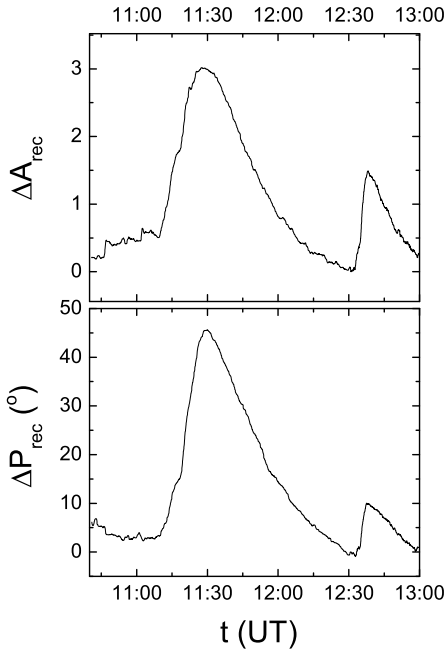


Figure 2 Time dependencies of the signal amplitude $A_{\rm rec}$ (upper panel) and phase $P_{\rm rec}$ (bottom panel) changes recorded by the AWESOME receiver located in Belgrade (Serbia) during presence of the solar X-ray flare that occurred on May 5, 2010.

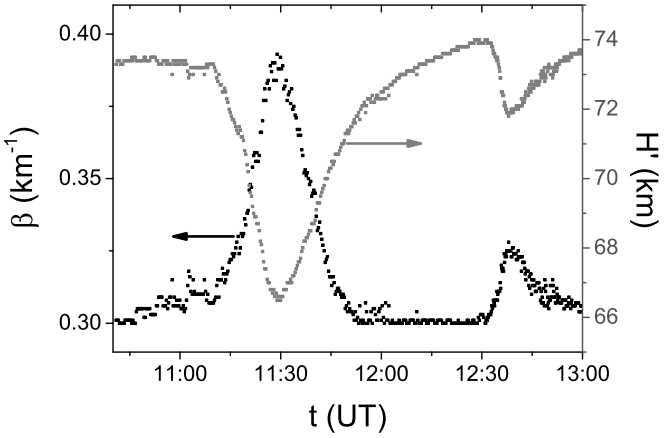


Figure 3 Time dependencies of the calculated Wait's parameters β and H' during presence of the solar X-ray flares that occurred on April 22, 2011.

based our analysis of the D-region on data obtained by radio sounding using the 23.4 kHz VLF signal emitted by the DHO transmitter located in Rhauderfehn (Germany) and received at Institute of Physics in Belgrade (Serbia). The transmitter was used in many of our studies (see, for example, Todorović Drakul et al. 2016 and reference therein) because it provides the best quality suitable signal frequency for the location of the receiver, and has a relatively short signal propagation path.

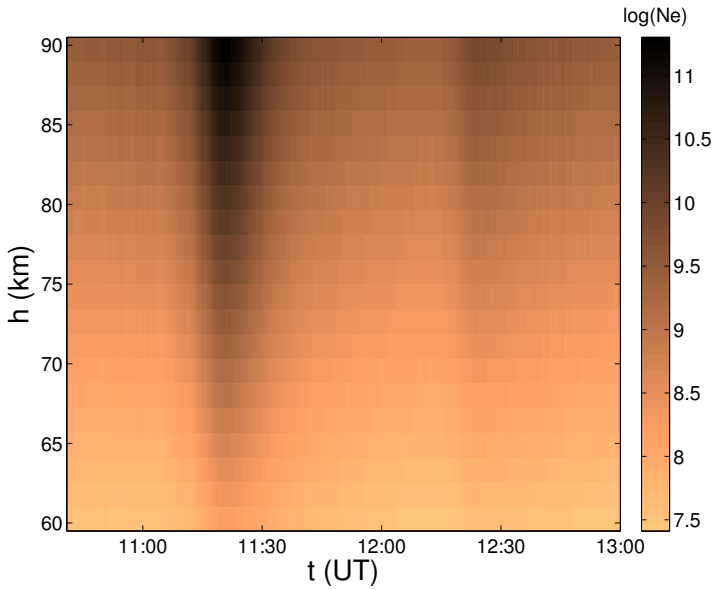


Figure 4 Time and altitude dependencies of the D-region electron density $N_e^* = N_e/1m^3$.

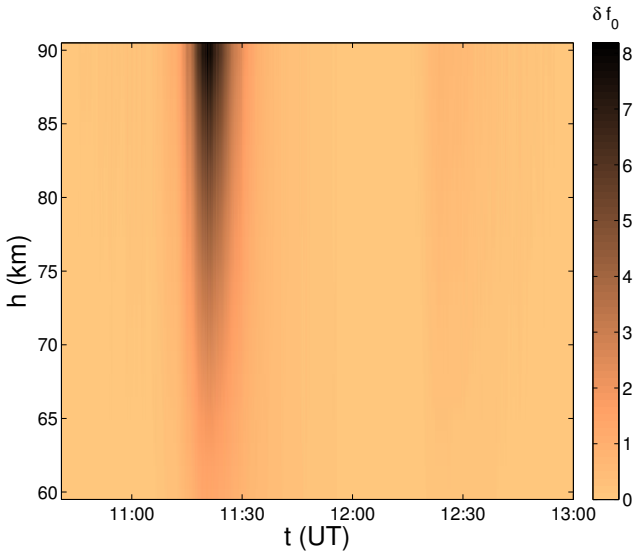


Figure 5 Time and altitude dependencies of the relative changes of electron plasma frequency during perturbation with respect to its values during quiet conditions.

According to the above relation (Eq. (1)), the obtained pairs of Wait's parameters are time dependent, $\beta = \beta(t)$ and $H' = H'(t)$, as presented in Fig. 3 for the considered cases.

The altitude and temporal dependencies of the resulting modeled electron density by Eq. 2 are shown in Fig. 4. Here it can be seen that the most pronounced electron density increase at fixed altitude h occurs at the time of the electron density maximum when it rises by more than one order of magnitude. The maximum increase relative to the initial value is obtained at 90 km.

The electron plasma frequency changes described by Eq. (4) are presented in Fig. 5. We can see that these variations are more pronounced during the first, stronger, influences of X radiation.

Finally, time evolutions of the total electron content (TEC) calculated from Eq. 5 (restricted on the D-region) are shown in Fig. 6. As in the pervious analysis this value has significant increase: it reaches near 10^{-2} TECU and about 5×10^{-4} TECU started from the values of about 2×10^{-4} TECU. Comparing these values we obtained an increase of nearly 5000% and 170%, respectively.

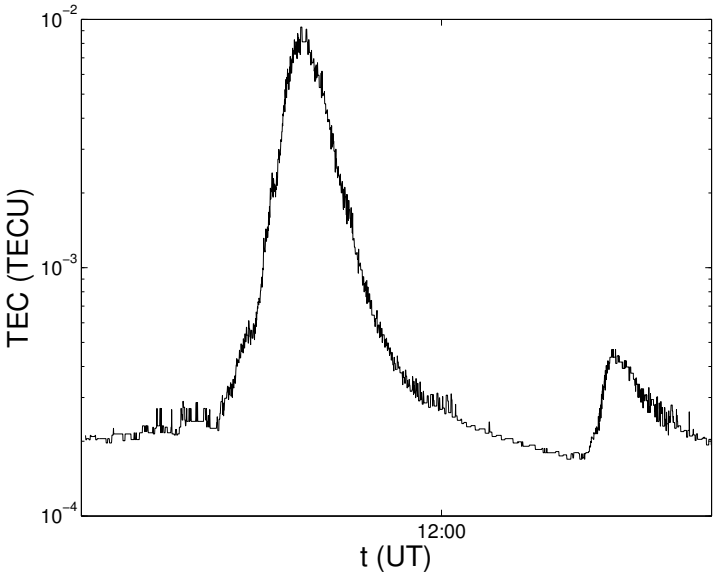


Figure 6 Time evolution of the TEC during the considered period.

Summary

In this paper we investigated the ionospheric disturbances induced by solar X-ray flares. Our attention was focused on D-region plasma parameters calculated from the ionospheric monitoring by VLF radio wave. The obtained results for two considered X-ray flares of classes C7.7 and C3.0 show that:

- The electron density in the D-region has a large increase during solar X-ray influences in both cases. This increase is larger in the first case than in the second one which is expected because of more intensive X-radiation during first event than during second one.
- The critical frequency relative changes with respect to its values during quite conditions are significantly larger in the first case when the intensity of X-radiation was stronger than in the second case.
- Time evolution of the TEC shows a rise of nearly two orders of magnitude and within the same order of magnitude in the first and second perturbed period, respectively.

These results show that the D-region is significantly disturbed by the X-ray flares of class C, contrary to the plasma located in the upper ionosphere. Consequently, we can conclude that the influence of this phenomenon is more important for the lower than for the upper ionospheric investigation as well as for simulation of radio waves propagation at altitudes below about 100 km in the case of no strong flares.

Acknowledgment The author would like to thank the Ministry of Education, Science and Technological Development of the Republic of Serbia for the support of this work within the projects III-44002 and 176002. The author is also grateful to Vladimir

M. Čadež for very useful suggestions and comments. The data for this paper collected by GOES-15 satellite is available at NOAA's National Centers for Environmental information (http://satdat.ngdc.noaa.gov/sem/goes/data/new_full/2011/04/goes15/csv/g15_xrs_2s_20110422_20110422.csv). Requests for the VLF data used for analysis can be directed to the corresponding author.

References

Bajčetić J., Nina A., Čadež V. M. and Todorović B. M. (2015) Therm. Sci. 19, Suppl. 2, S229.

Chau J. L., Röttger J. and Rapp M. (2014) J. Atmos. Sol.-Terr. Phys. 118, 113.

Cohen M., Inan U. and Paschal E. W. (2010) IEEE T. Geosci. Remote. 48, 3.

Ferguson J. A. (1998) Computer Programs for Assessment of Long-Wavelength Radio Communications, Version 2.0, Space and Naval Warfare Systems Center, San Diego.

Grubor D. P., Šulić D. M. and Žigman V. (2005) Serb. Astron. J. 171, 29.

Grubor D. P., Šulić D. M. and Žigman V. (2008) Ann. Geophys. 26, 1731.

Hofmann-Wellenhof B., Lichtenegger H. and Collins J. (2001) Global Positioning System: Theory and Practice, Springer-Verlag, New York.

Jakowski N., Stankov S. M., Klaehn D. (2005) Ann. Geophys. 23(9), 3071.

Jilani K., Mirza A. M. and Khan T. A. (2013) Astrophys. Space Sci. 344, 135.

Kolarski A. and Grubor D. (2014) Adv. Space Res. 53(11), 1595.

Nina A., Čadež V., Srećković V. A. and Šulić D. (2011) Balt. Astron. 20, 609.

Nina A., Čadež V., Srećković V. and Šulić D. (2012a) Nucl. Instrum. Methods in Phys. Res. B 279, 110.

Nina A., Čadež V., Šulić D., Srećković V. and Žigman V. (2012b) Nucl. Instrum. Methods in Phys. Res. B 279, 106.

Nina A. and Čadež V. M. (2013) Geophys. Res. Lett. 40(18), 4803.

Nina A. and Čadež V. M. (2014) Adv. Space Res. 54(7), 1276.

Nina A., Simić S., Srećković V. and Popović L. Č. (2015a) Geophys. Res. Lett. 42(19), 8250.

Nina A., Čadež V. M. and Bajčetić J. (2015b) Serb. Astron. J. 191, 51.

Schmitter E. D. (2013) Ann. Geophys. 31(4), 765.

Shim Ja. S. (2009) Analysis of Total Electron Content (TEC) Variations in the Low- and Middle-Latitude Ionosphere, PhD Dissertation, Utah State University, Logan, Utah.

Singh R., Veenadhari B., Maurya A. K., Cohen M. B., Kumar S., Selvakumaran R., Pant P., Singh A. K. and Inan U. S. (2011) J. Geophys. Res.-Space 116, 10301.

Singh A. K., Singh A., Singh R. and Singh R. (2014) Astrophys. Space Sci. 350(1), 1.

Stankov S.M., Stegen K., Muhtarov P. and Warnant R. (2011) Adv. Space Res. 47(7), 1172.

Strelnikova I. and Rapp M. (2010) Adv. Space Res. 45(2), 247.

Thomson N. R. (1993). J. Atmos. and Sol.-Terr. Phys. 55, 173.

Todorović Drakul M., Čadež V. M., Bajčetić J., Popović L. Č., Blagojević D. and Nina A. (2016) Serb. Astron. J. doi: 10.2298/SAJ160404006T.

Verhulst T.G.W., Sapundjiev D., Stankov S. M. (2016) Adv. Space Res. 57, 11, 2407.
Wait J. R. and Spies K. P. (1964) Characteristics of the Earth-ionosphere waveguide for VLF radio waves, NBS Technical Note 300, National Bureau of Standards, Boulder, CO.
Xiong B., Wan W., Liu L., Withers P., Zhao B., Ning B., Wei Y., Le H., Ren Z., Chen Y., He M. and Liu J. (2011) J. Geophys. Res. 116, A11317.